

3D NANOPROCESSING OF FUNCTIONAL MATERIALS

Liudmila A. Pozhar

Oak Ridge National Laboratory, Oak Ridge, TN
University of Tennessee, Knoxville, TN
and

Michael Z.-C. Hu

Oak Ridge National Laboratory, Oak Ridge, TN

CONTENTS

1. **STATISTICAL MECHANICS – MD SYNERGY: “NANOMATERIALS BY DESIGN” APPROACH.**
2. **POZHAR-GUBBINS (PG) APPROACH IN NON-EQUILIBRIUM STATISTICAL MECHANICS: PREDICTION OF NON-EQUILIBRIUM PHYSICAL PROPERTIES AND PROCESS EQUATIONS.**
3. **EQUILIBRIUM STATISTICAL MECHANICS AND EMD: STRUCTURE AND STATISTICAL PROPERTIES.**
4. **NEMD: PREDICTION EVALUATION.**
5. **CONCLUSIONS**

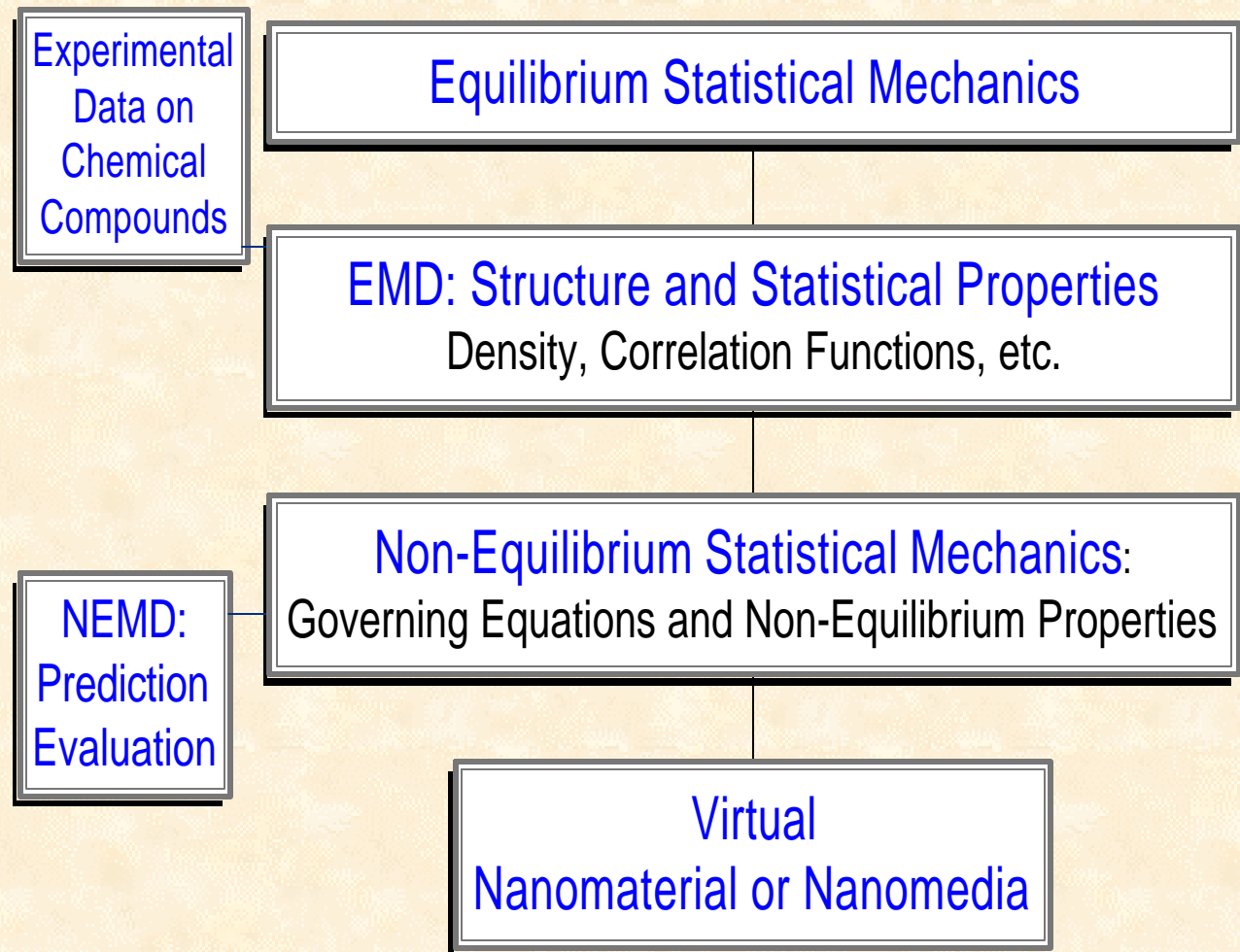
MAJOR REFERENCES

1. L.A. Pozhar, *Transport Theory of Inhomogeneous Fluids* (World Scientific, New Jersey, 1994);
2. L.A. Pozhar, *Phys. Rev. E* **61**, 1432 (2000).
3. L.A. Pozhar and K.E. Gubbins, *Phys. Rev. E* **56**, 5367 (1997); *Ibid.*, **94**, 1367 (1991).
4. L.A. Pozhar, *Ukrainian Phys. J.* **34**, 779 (1989) (in Russian).
5. J.M.D. MacElroy, L.A. Pozhar and S.-H. Suh, *Colloids and Interfaces A* **187-188**, 493 (2001).
6. J.K. Percus, L.A. Pozhar, and K.E. Gubbins, *Phys. Rev. E* **51**, 261 (1995); L.A. Pozhar, K.E. Gubbins, and J.K. Percus, *Phys. Rev. E* **48**, 1819 (1993).

OAK RIDGE NATIONAL LABORATORY
U. S. DEPARTMENT OF ENERGY

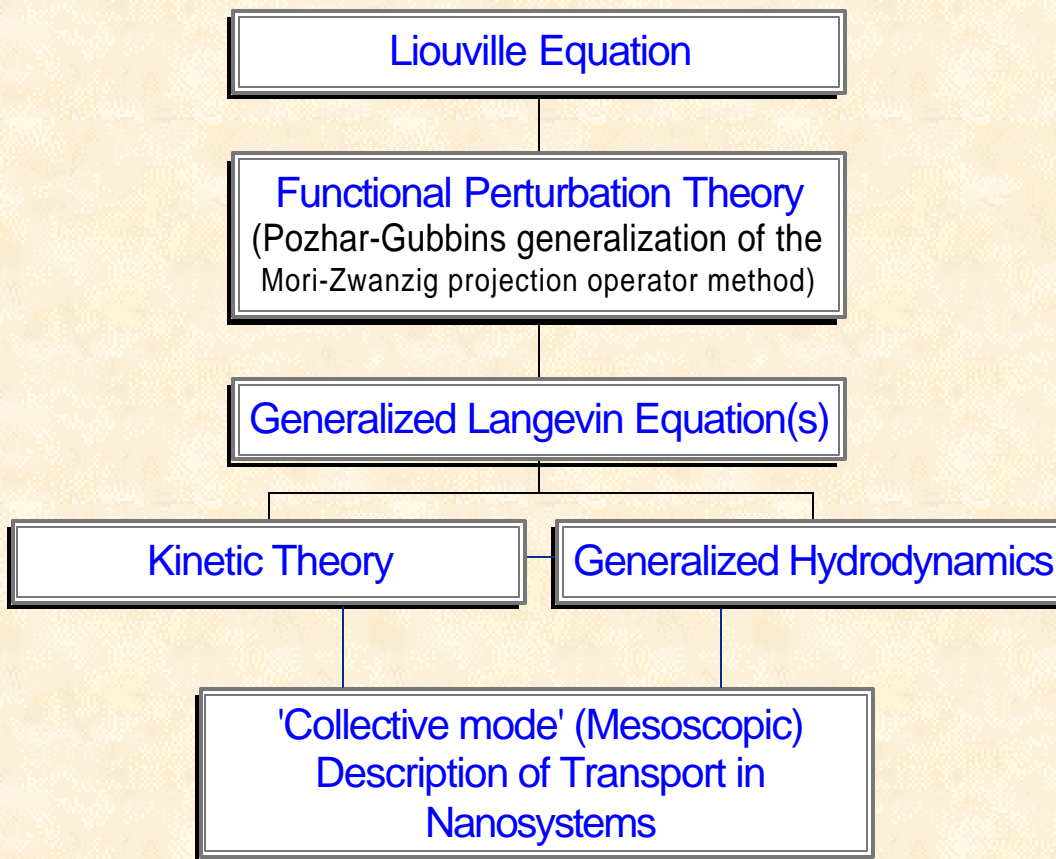


VIRTUAL FABRICATION CYCLE



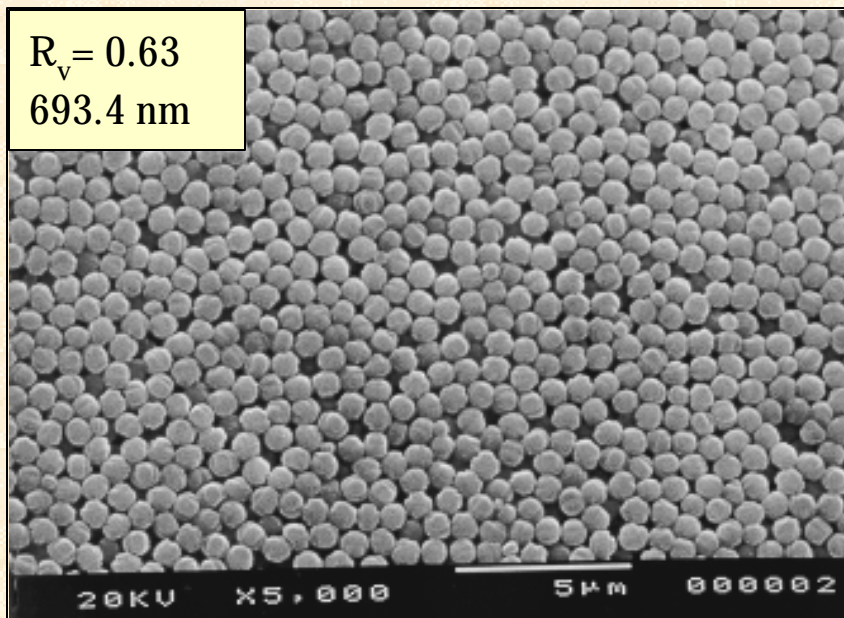
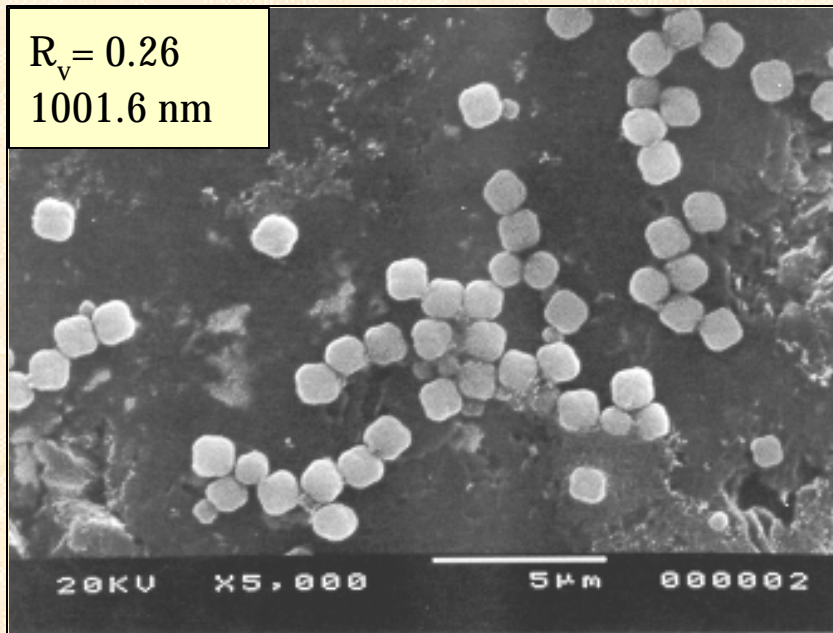
2. PG-APPROACH IN NON-EQUILIBRIUM STATISTICAL MECHANICS: PREDICTION OF NON-EQUILIBRIUM PHYSICAL PROPERTIES AND PROCESS EQUATIONS

THE STRUCTURE OF THE PG-APPROACH



EXPERIMENTAL SYSTEMS

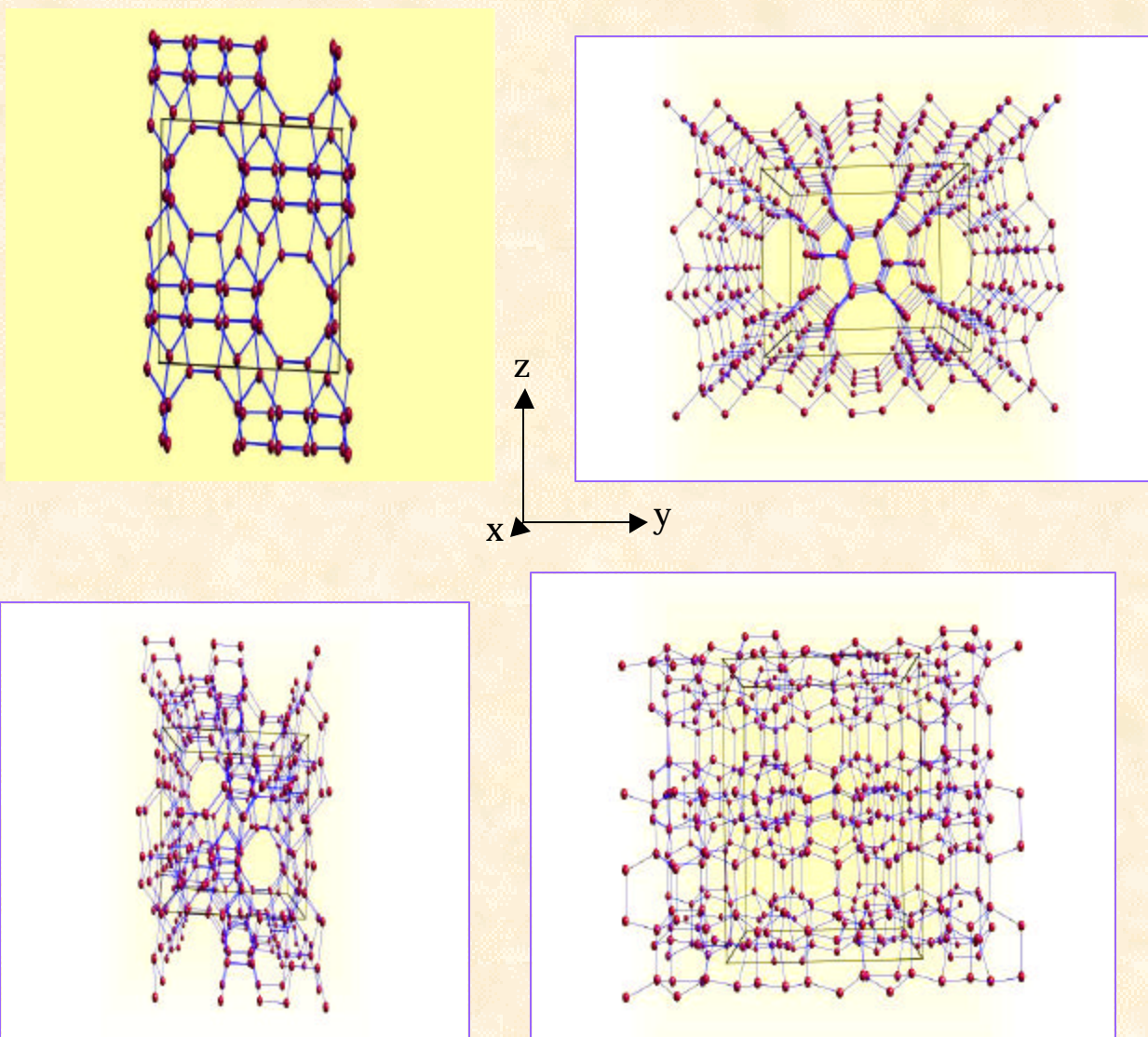
Silicate-1 Synthesis (Temp = 150°C)



OAK RIDGE NATIONAL LABORATORY
U. S. DEPARTMENT OF ENERGY



2D and 3D - images of various faces of zeolite crystals reconstructed from HRTEM-based diffraction patterns using “Crystal Maker” software (the black box in the center of each image represents the unit cell).



EXAMPLE 1: PG-theoretical diffusion in nanosystems

$$\hat{\mathbf{D}}_T(\mathbf{q}) = \frac{3t_d(\mathbf{q})}{2\mathcal{S}^2 n_1(\mathbf{q})} \sqrt{\frac{p\mathbf{b}}{m}} \hat{\mathbf{D}}(\mathbf{q}), \quad (1)$$

$$t_d^{-1}(\mathbf{q}) = \int d\hat{\mathbf{s}} n(\mathbf{q} - \mathcal{S}\hat{\mathbf{s}}) g(\mathbf{q}, \mathbf{q} - \mathcal{S}\hat{\mathbf{s}}) + \frac{\sqrt{2}\mathcal{S}_{fw}^2}{\mathcal{S}^2} \int d\hat{\mathbf{s}} n_w(\mathbf{q} - \mathcal{S}_{fw}\hat{\mathbf{s}}) g_{fw}(\mathbf{q}, \mathbf{q} - \mathcal{S}_{fw}\hat{\mathbf{s}})$$

\mathbf{q} - a position within the fluid; \mathcal{S} , \mathcal{S}_w and \mathcal{S}_{fw} - the effective diameters of the hard-core contributions to the potentials of intermolecular interactions of the fluid molecules, wall molecules, and fluid and wall molecules, respectively; $\mathbf{b} = 1/k_B T$, k_B is the Boltzmann constant, T is temperature, m is the mass of a fluid molecule; $n_1(\mathbf{q})$, $n(\mathbf{q})$ and $n_w(\mathbf{q})$ are the equilibrium number densities of the tracer "component" 1, the fluid "mixture" and the walls, respectively; g and g_{fw} are the contact values of the equilibrium fluid-fluid and fluid-wall pair correlation functions (PCFs), respectively, and the integrals are over the surface of the unit sphere ($\hat{\mathbf{o}}$ is the unit vector).

The Cartesian tensor $\mathbf{D}(\mathbf{q})$ in Eq. (1) has the form.

$$\hat{\mathbf{D}}(\mathbf{q}) = \frac{1}{\mathbf{b}} [\mathbf{I} + \mathbf{F}\{n\}] \quad (2)$$

\mathbf{I} is the unit matrix; $\mathbf{F}\{n\}$ is a functional of the fluid density and composition.

The mass flux of the component 1 is:

$$\begin{aligned} \mathbf{J}_1(\mathbf{q}) &= -n_1(\mathbf{q}) \hat{\mathbf{D}}_T(\mathbf{q}) \cdot \frac{\nabla n_1(\mathbf{q})}{\nabla \mathbf{q}} \\ &= -n_1(\mathbf{q}) D_T(\mathbf{q}) \frac{\nabla n_1(\mathbf{q})}{\nabla \mathbf{q}} \end{aligned}$$

$\mathbf{d}n_1(\mathbf{q})$ is the deviation of the nonequilibrium number density of the component 1 from its equilibrium value, $n_1(\mathbf{q})$.

$$D_T(\mathbf{q}) = \frac{3t_d(\mathbf{q})}{2s^2 n_1(\mathbf{q})} \sqrt{\frac{\mathbf{p}}{mb}}$$

The zero-order approximation to the self-diffusion coefficient measured experimentally,

$$D_P(\mathbf{q}) = n_1(\mathbf{q}) D_T(\mathbf{q})$$

$$= \frac{3}{2s^2} \sqrt{\frac{\mathbf{p}}{mb}} t_d(\mathbf{q})$$

$$= \frac{\frac{3}{2s^2} \sqrt{\frac{\mathbf{p}}{mb}}}{\left[\int d\hat{\mathbf{s}} n(\mathbf{q} - \mathbf{s}\hat{\mathbf{s}}) g(\mathbf{q}, \mathbf{q} - \mathbf{s}\hat{\mathbf{s}}) + \frac{\sqrt{2}s^2}{s^2} \int d\hat{\mathbf{s}} n_w(\mathbf{q} - \mathbf{s}_{fw}\hat{\mathbf{s}}) g_{fw}(\mathbf{q}, \mathbf{q} - \mathbf{s}_{fw}\hat{\mathbf{s}}) \right]}$$

Introducing the notations:

$$D_P^{ff}(\mathbf{q}) = \frac{3}{2s^2} \sqrt{\frac{\mathbf{p}}{mb}} \frac{1}{\int d\hat{\mathbf{s}} n(\mathbf{q} - \mathbf{s}\hat{\mathbf{s}}) g(\mathbf{q}, \mathbf{q} - \mathbf{s}\hat{\mathbf{s}})}$$

$$D_P^{fw}(\mathbf{q}) = \frac{3}{4s_{fw}^2} \sqrt{\frac{2\mathbf{p}}{mb}} \frac{1}{\int d\hat{\mathbf{s}} n_w(\mathbf{q} - \mathbf{s}_{fw}\hat{\mathbf{s}}) g_{fw}(\mathbf{q}, \mathbf{q} - \mathbf{s}_{fw}\hat{\mathbf{s}})}$$

one can rewrite the above equation in the familiar form

$$\frac{1}{D_P(\mathbf{q})} = \frac{1}{D_P^{ff}(\mathbf{q})} + \frac{1}{D_P^{fw}(\mathbf{q})}$$

Introducing dimensionless quantities:

$\mathbf{q}^* = \mathbf{q}/s_w$, $n^*(\mathbf{q}^*) = s_w^3 n(\mathbf{q}^*)$, $n_w^*(\mathbf{q}^*) = s_w^3 n_w(\mathbf{q}^*)$, and

$D_P^*(\mathbf{q}^*) = D_P(\mathbf{q}^*)/D^0$, $D_P^{ff*}(\mathbf{q}^*) = D_P^{ff}(\mathbf{q}^*)/D^0$ and $D_P^{fw*}(\mathbf{q}^*) = D_P^{fw}(\mathbf{q}^*)/D^0$

where

$D^0 = \frac{3}{2} \sqrt{\frac{\mathbf{p}}{b_m}} s_w$, one has:

$$D_P^{ff*}(\mathbf{q}^*) = \frac{s_w^2}{s^2 \int d\hat{\mathbf{s}} n^*(\mathbf{q}^* - \frac{\mathbf{s}}{s_w} \hat{\mathbf{s}}) g(\mathbf{q}^*, \mathbf{q}^* - \frac{\mathbf{s}}{s_w} \hat{\mathbf{s}})'} ,$$

$$D_P^{fw*}(\mathbf{q}^*) = \frac{s_w^2}{\sqrt{2} s_{fw}^2 \int d\hat{\mathbf{s}} n_w^*(\mathbf{q}^* - \frac{\mathbf{s}_{fw}}{s_w} \hat{\mathbf{s}}) g_{fw}(\mathbf{q}^*, \mathbf{q}^* - \frac{\mathbf{s}_{fw}}{s_w} \hat{\mathbf{s}})'} ,$$

EXAMPLE 2: PG-theoretical shear viscosity of slit pore nanosystems

$$h(z) = h_b \{ 4p n^*(z) t_h^*(z) [1 + pb^{*0}(z)]^2 + (16/5)pn^*(z) b^{*0}(z) \},$$

NOTATIONS:

$h(z)$ – PG-theoretical viscosity; $h_b = (5/16 s^2) (m / p b_B)^{1/2}$, $b_B = 1/(k_B T)$, k_B - the Boltzmann constant, T - temperature, m - the mass of a fluid molecule, s and s_{fw} - the diameters of the hard-core parts of the fluid-fluid and fluid-wall intermolecular interaction potentials, respectively; $n^*(z) = n(z)s^3$ and $n_w^*(z) = n_w(z)s_{fw}^3$ - the dimensionless equilibrium number densities, $n(z)$ and n_w , of the nanofluid and the confinement; $g(z, z - s \cos q)$ and $g_{fw}(z, z - s_{fw} \cos q)$ - the contact values of the equilibrium fluid-fluid and fluid-wall pair correlation function contact values, respectively; and q is the angle between the vector connecting the centres of mass of the interacting molecules and the positive z -direction.

$$t_h^*(z) = \{ 2p [n^*(z) + (1/3) n_1^*(z) + \sqrt{2} n_2^*(z)] \}^{-1}$$

$$n^*(z) = \int_0^p dq \sin q n^*(z - s \cos q) g(z, z - s \cos q),$$

$$n_1^*(z) = \int_0^p dq \sin q [n^*(z - s \cos q) - n^*(z)] g(z, z - s \cos q),$$

$$n_2^*(z) = \int_0^p dq \sin q n_w^*(z - s_{fw} \cos q) g_{fw}(z, z - s_{fw} \cos q),$$

$$b^{*0}(z) = \int_0^p dq \sin^3 q \cos^2 q n^*(z - s \cos q) g(z, z - s \cos q).$$

3. PG - THEORY + EMD

A) SELF-DIFFUSION

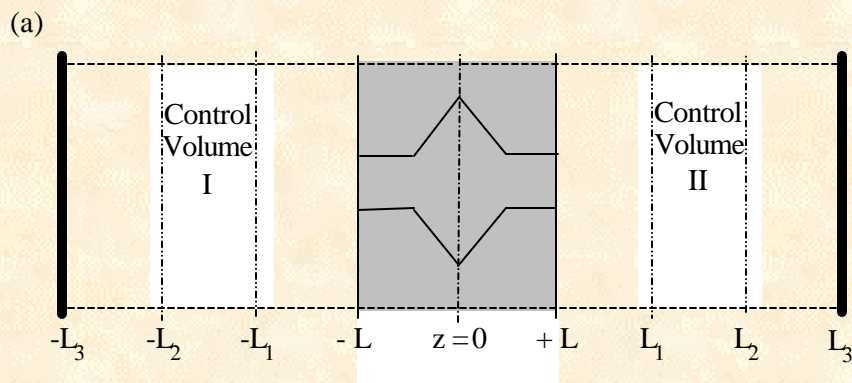
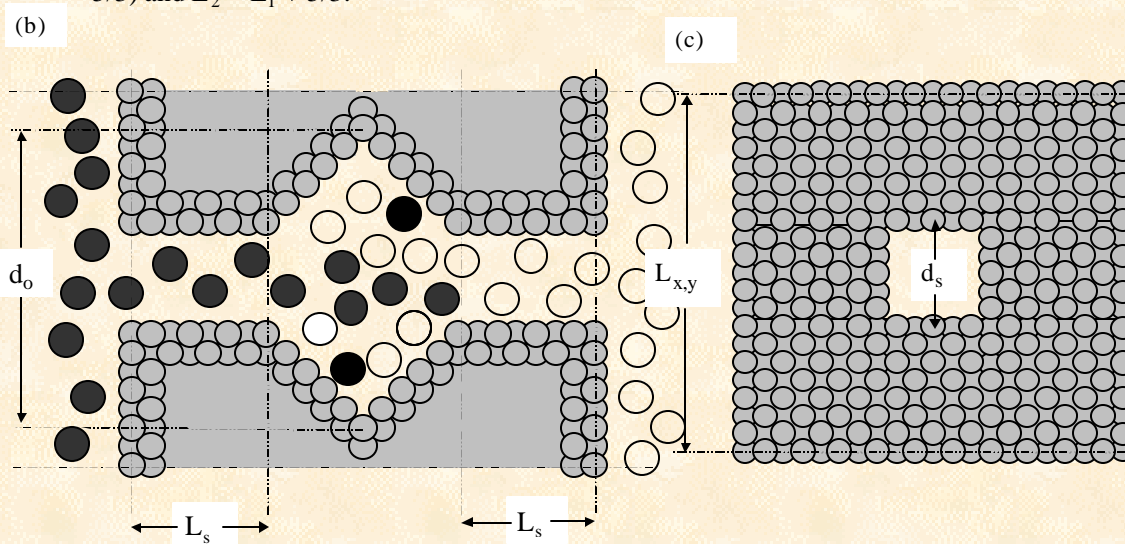


Figure 1. Model system studied in this work by the PG-theoretical and MD simulations means. (a) The fundamental cell (imaged in the x and z directions) with control volumes I and II; (b) side view of the nanopore system; (c) pore face. The axial half length, L , of the composite pore was $L_s + 2.5\sqrt{2}$; the square channel: $L_s = 3.5\sqrt{2}$; width: $d_s = 3\sqrt{2}$. The central unit (“octahedron”): maximum dimension $d_o = 8\sqrt{2}$. The pore system is composed of two dense face-centred cubic layers of immobile atoms. The bulk regions: $L_3 = \pm (18.5\sqrt{2} + L_s)$. Control volumes: $-L_2 < z < -L_1$; $L_1 < z < L_2$, where $L_1 = (10.5\sqrt{2} + L_s - 5/3)$ and $L_2 = L_1 + 5/3$.



SIMULATION CONDITIONS: DIFFUSION

$$\mathbf{f}_{ij}^{SF}(r_{ij}) = \mathbf{f}_{ij}(r_{ij}) - \mathbf{f}_{ij}(r_{cut}) - \left(\frac{d\mathbf{f}_{ij}(r_{ij})}{dr_{ij}} \right)_{r_{cut}} (r_{ij} - r_{cut}); \quad r_{ij} \leq r_{cut}$$

$$= 0; \quad r_{ij} > r_{cut}$$

with

$$\mathbf{f}_{ij}(r_{ij}) = 4\mathbf{e}_{ij} \left(\left(\frac{\mathbf{s}_{ij}}{r_{ij}} \right)^{12} - \left(\frac{\mathbf{s}_{ij}}{r_{ij}} \right)^6 \right),$$

Table 1. Parameters of the Lennard-Jones potentials.

Component pair	σ , Å	ϵ/k (K)
Fluid-fluid	3.817	148.2
Wall-wall	3.000	228.4
Fluid-wall	3.409	184.0

Fluid parameters: the average number density in the “bulk” volumes, $n^* = 0.5\mathbf{s}^3$, where \mathbf{s} is the LJ-diameter of the fluid particles; the dimensionless temperature, $T^* = k_B T / \mathbf{e} = 1.5$. The average number density of the confined nanofluid, $n_f^* = (0.4 \pm 0.04)\mathbf{s}^3$. **Note:** bulk fluid of similar potential parameters at this density and temperature possesses a pressure of about 220 atm; the self-diffusion coefficient for the model Lennard-Jones fluid in the bulk state has been independently determined using traditional EMD procedures to be $3.4 \times 10^{-4} \text{ cm}^2/\text{s}$.

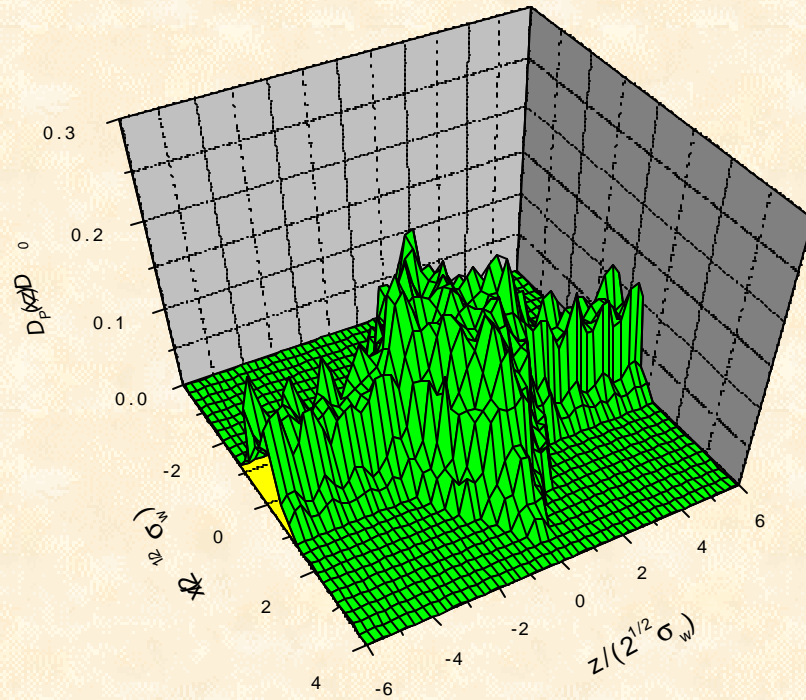


Figure 2. Zero-order approximation of the PG-theoretical self-diffusion coefficient for the entire pore system in the plane $y=0$.

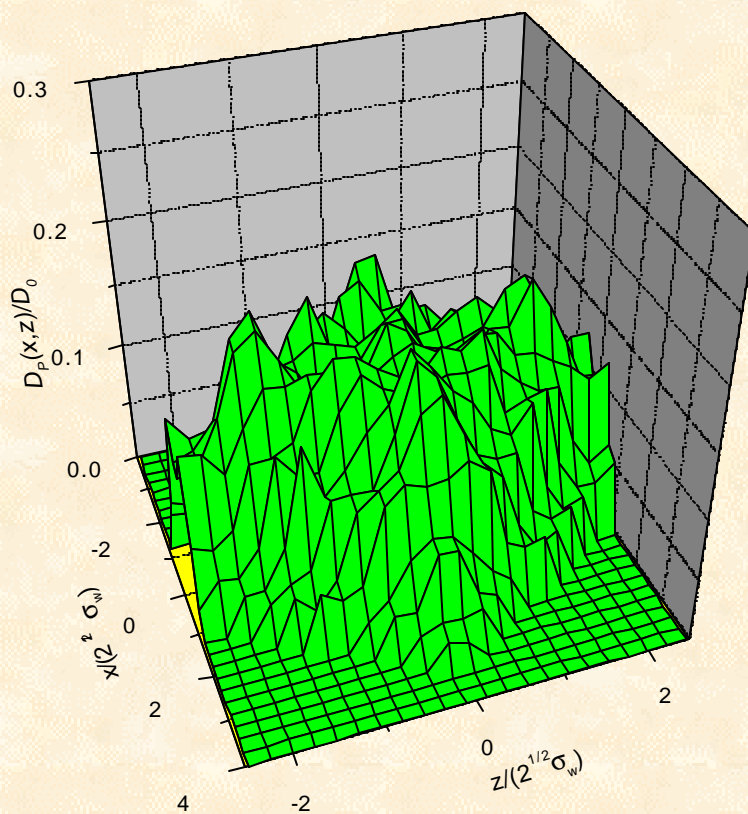


Figure 3. Zero-order approximation of the PG-theoretical self-diffusion coefficient for the central cross-section of the “octahedron” cavity at $y=0$

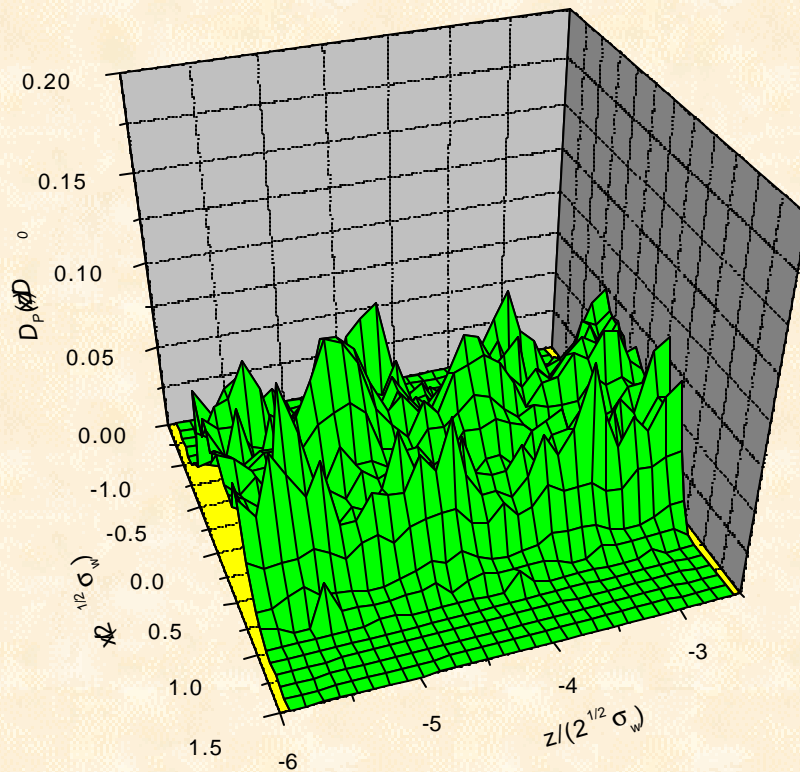


Figure 4. Zero-order approximation of the PG- theoretical self-diffusion coefficient for the square channel in the plane $y=0$

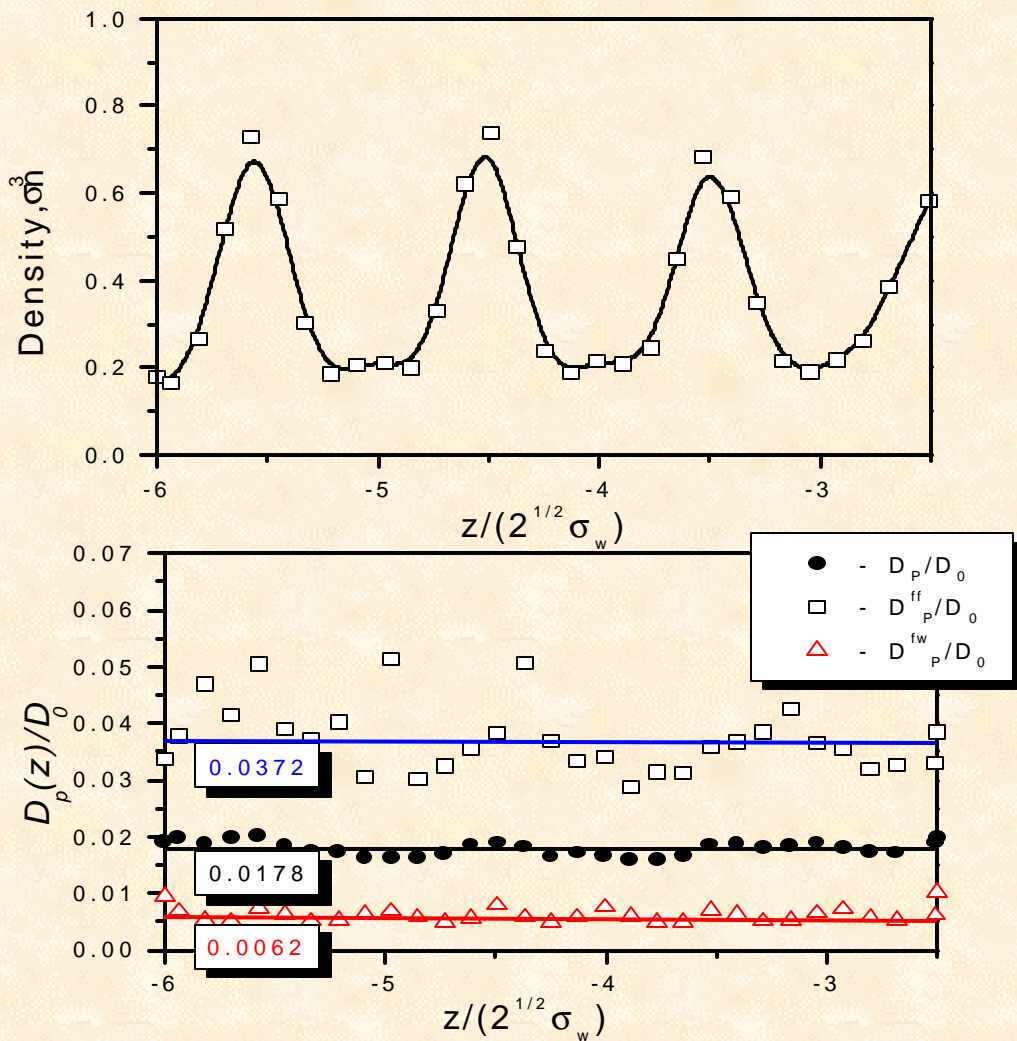


Figure 5. Top : the average nanofluid density (based on pore cross-section) for z-bins within the left square channel (open squares); the curve corresponds to a fit by B-splines.

Bottom: the fluid-fluid and fluid-wall contributions, D^{ff}_p/D^0 (open squares) and D^{fw}_p/D^0 (open triangles), respectively, to the zero-order approximation of the across-the-pore average of the PG-theoretical self-diffusion coefficient for the square channel. The horizontal lines correspond to the average values which in each case are $\langle D^{ff}_p/D^0 \rangle = 0.0372$; $\langle D^{fw}_p/D^0 \rangle = 0.0062$; and overall (the filled circles) $\langle D_p/D^0 \rangle = 0.0178$; $D^0 = 2.715 \times 10^{-3} \text{ cm}^2/\text{s}$.

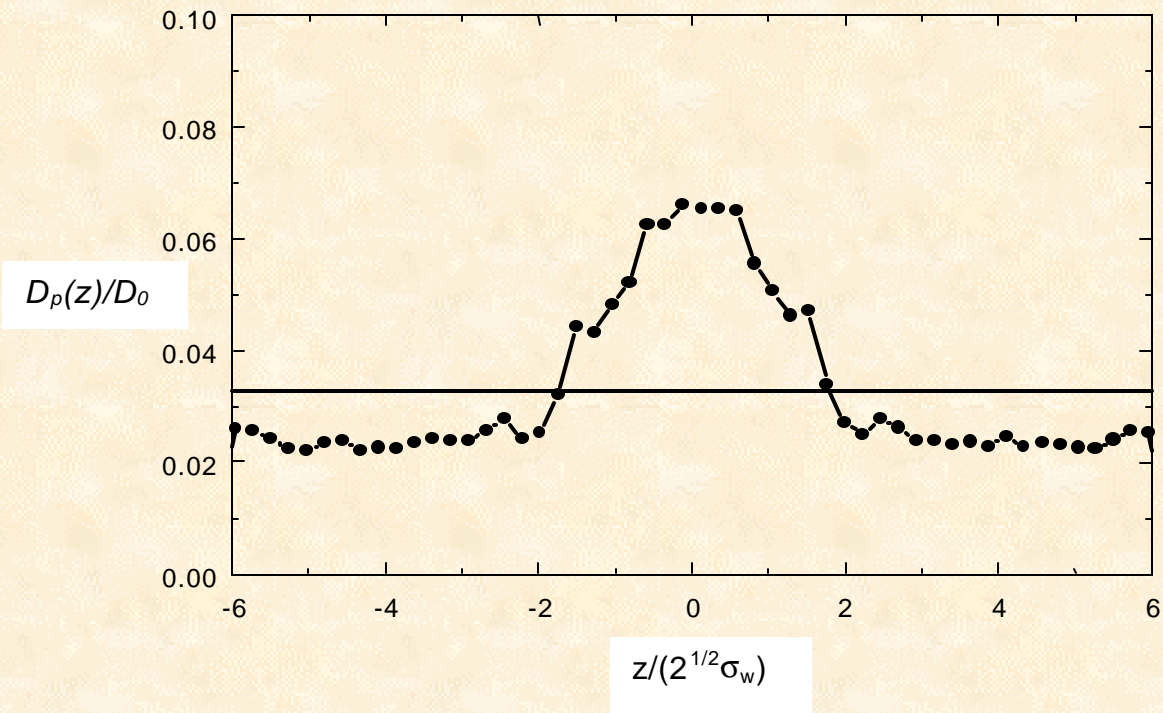


Figure 6. Zero-order approximation for the across-the-pore average of the PG-theoretical self-diffusion coefficient for the pore system. The horizontal line corresponds to the overall average value of the theoretical self-diffusion coefficient; $D^0= 2.715\times 10^{-3}$ cm²/s.

PG-THEORY + EMD
B) SHEAR VISCOSITY OF SLIT PORE NANOFUIDS

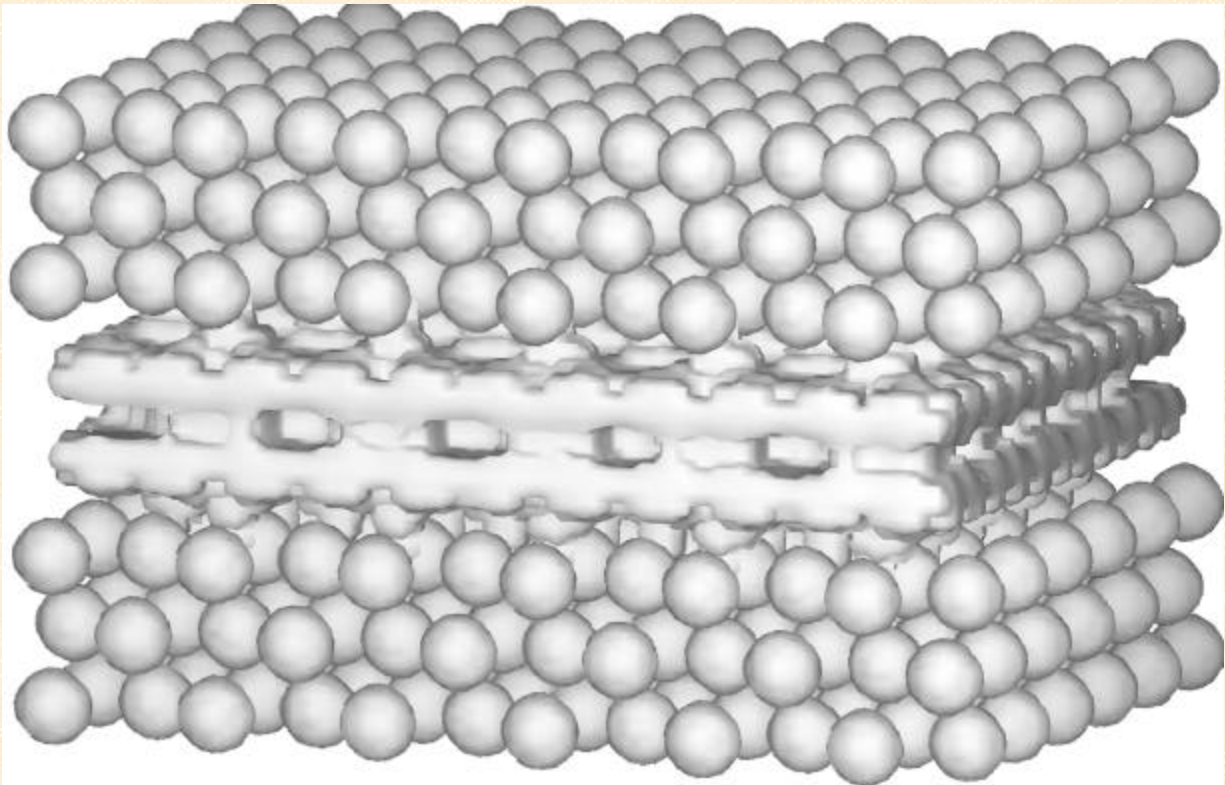


Figure 7. A model Lennard-Jones (LJ) nanofluid in a slit nanopore of $H=3.2s$ in width composed of immobile wall atoms: 3D image of the nanofluid number density, n_s^3 , where s is the effective diameter of nanofluid atoms. The average nanofluid density $\langle n_s^3 \rangle = 0.603$, temperature $k_B T/e = 0.958$; e - the energy parameter of the LJ potential.

Simulation Conditions

Intermolecular Interaction Potentials:

$$\mathbf{j}_{WCA}(r) = \begin{cases} 4\mathbf{e} \left[\left(\frac{\mathbf{s}}{r} \right)^{12} - \left(\frac{\mathbf{s}}{r} \right)^6 \right] + \mathbf{e}, & 0 < r < 2^{1/6} \mathbf{s}; \\ 0, & r \geq 2^{1/6} \mathbf{s}; \end{cases}$$

$$\mathbf{j}_{LJ}(r) = 4\mathbf{e} \left[\left(\frac{\mathbf{s}}{r} \right)^{12} - \left(\frac{\mathbf{s}}{r} \right)^6 \right], \quad r > 0.$$

System Parameters

Pore width, H/s	Fluid average number density, $n\mathbf{s}^3$	Temperature, $k_B T/e$	Simulation box sizes, $L_x/s = L_y/s$	Parameter a/σ	Parameter b/σ	Number of fluid particles N_f
3.2	0.442	0.729	13.026	2.368	0.638	240
	0.442	0.729	11.152	2.028	0.870	176
	0.442	0.729	10.636	1.933	0.958	160
	0.603	0.958	11.152	2.028	0.870	240
4.1	0.442	0.729	12.866	2.339	0.654	300
	0.603	0.958	12.894	2.344	0.651	411
5.1	0.442	0.729	12.637	2.298	0.678	360
	0.603	0.958	10.820	1.967	0.924	360
7.0	0.442	0.729	12.456	2.265	0.698	480
	0.603	0.958	10.664	1.934	0.952	480

$\mathbf{e} = \mathbf{s} = \mathbf{s}_w = m = 1$; the average wall density: $n_w^* = 0.850$; the number of wall atoms: 432; time steps: 2×10^{-5} and 2×10^{-4} .

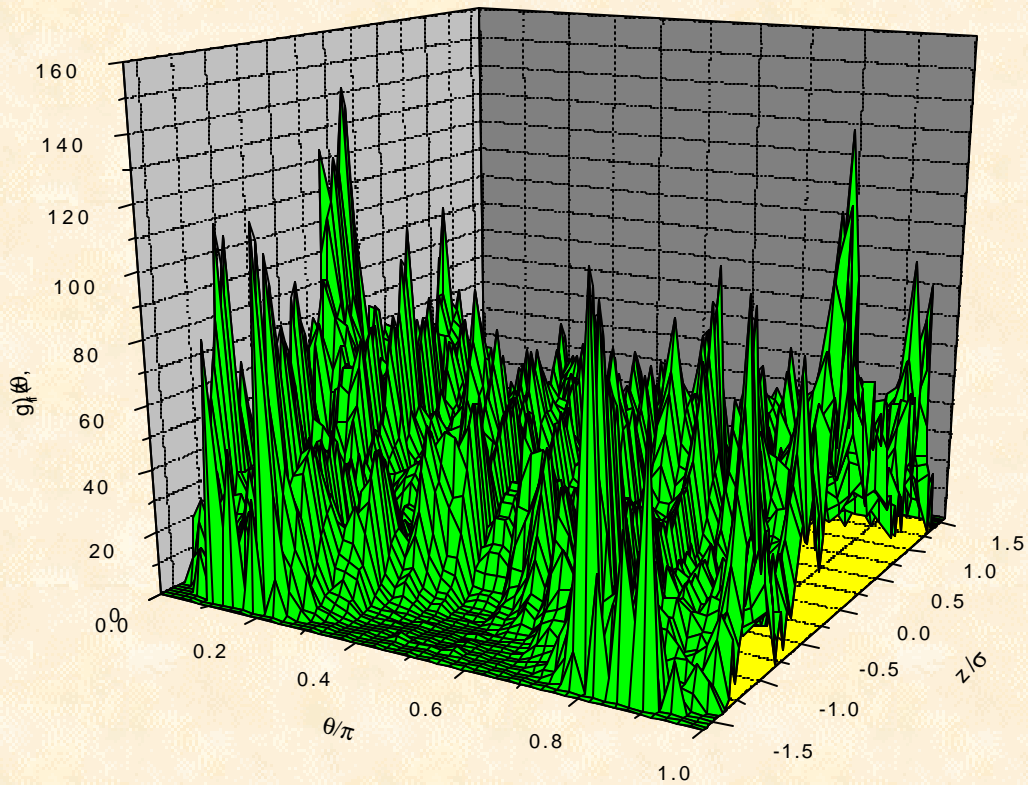


Figure 8. The fluid-fluid PCF contact values for the LJ nanofluid confined in a slit nanopore of $H=3.2\sigma$ in width. The average fluid density $\langle n\sigma^3 \rangle = 0.603$ and temperature $k_B T/e=0.958$.

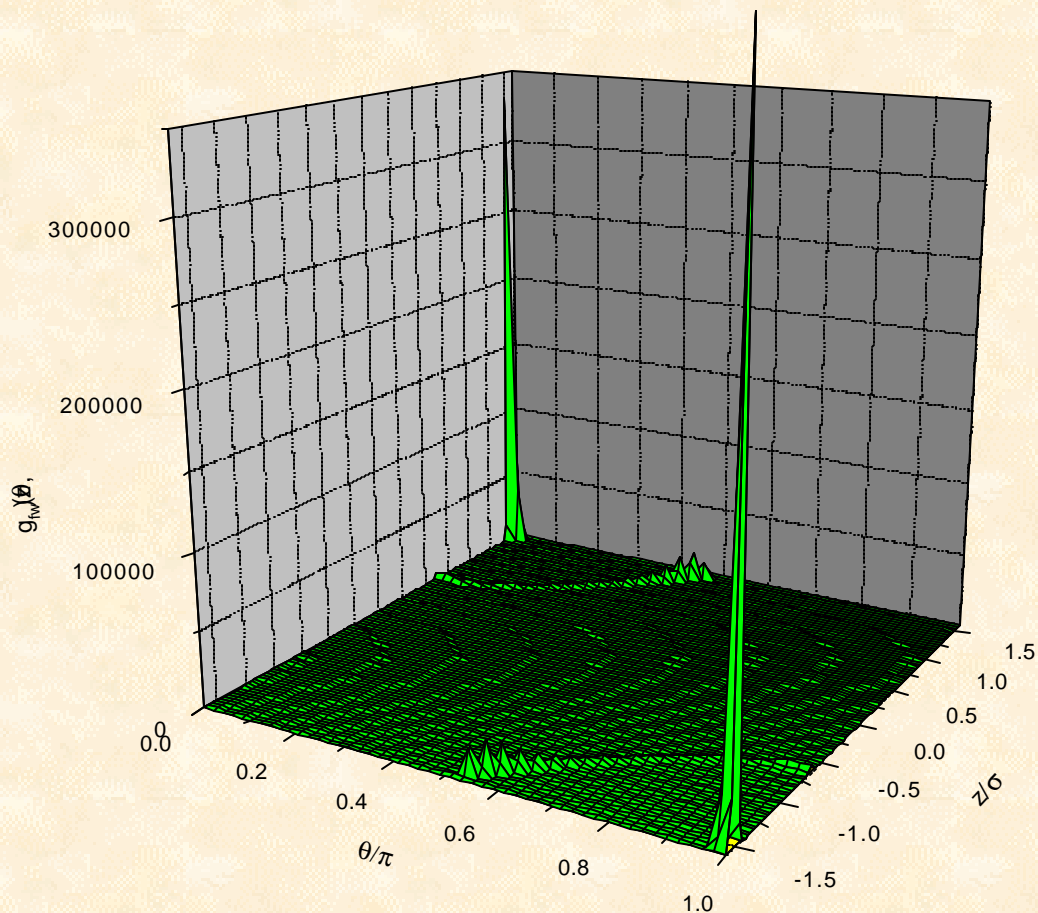


Figure 9. The fluid-wall PCF contact values for the LJ nanofluid confined in a slit nanopore of $H=3.2\sigma$ in width. The average fluid density $\langle n\sigma^3 \rangle = 0.603$ and temperature $k_B T/\epsilon=0.958$. Here θ is the angle between the vector connecting the centers of mass of a pair of fluid and wall molecules and the positive y -direction along the pore wall.

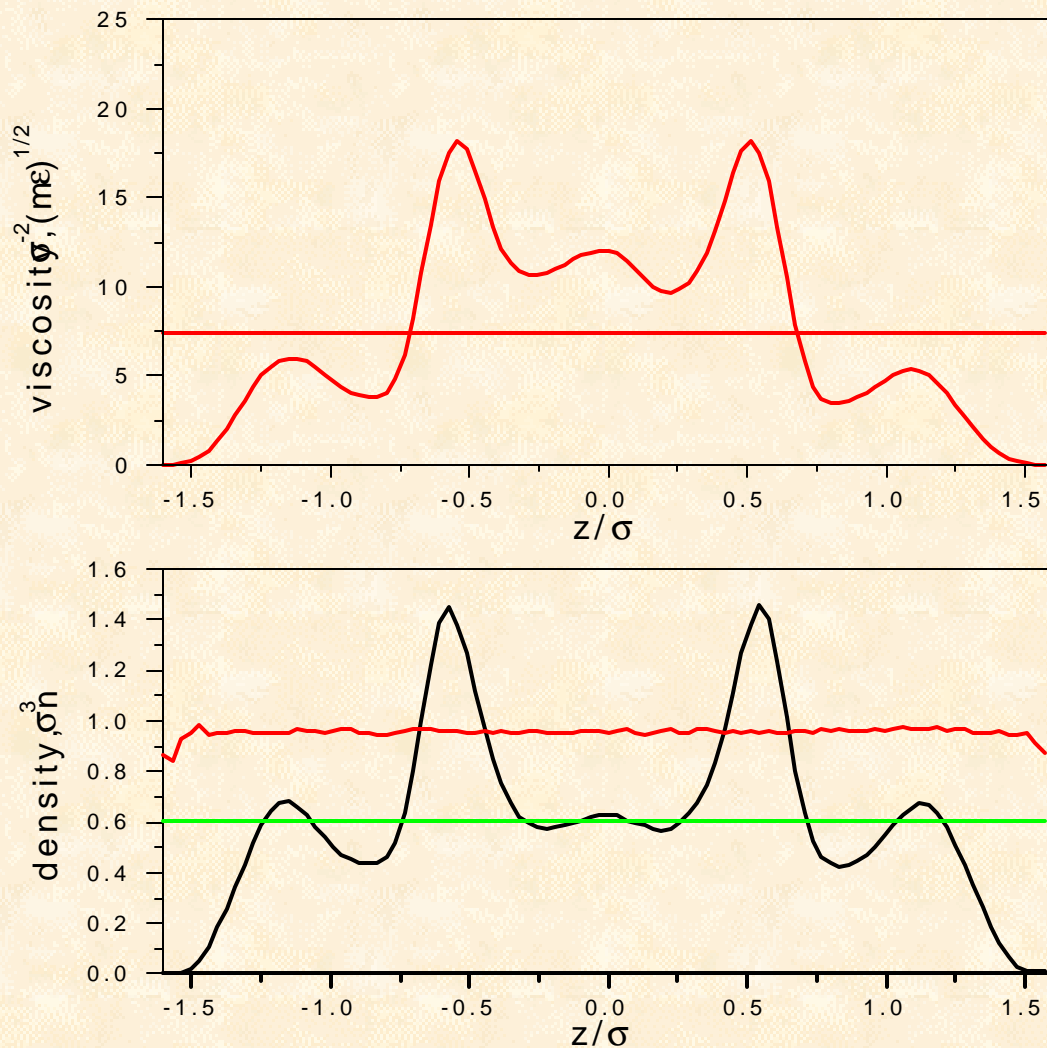


Figure 10. Top: the PG-theoretical viscosity for the LJ fluid confined in the pore of $H=3.2$ in width at $\langle n^3 \rangle = 0.603$ and temperature $k_B T/\epsilon=0.958$. Curve: reduced PG-theory with the EMD-simulated PCFs. Straight line: the corresponding pore-average PG-theoretical viscosity. Bottom: the corresponding number density (curve), average number density (lower line) and temperature (upper line).

4. NEMD SIMULATIONS AND COMPARISON OF THE RESULTS

A) SELF-DIFFUSION

The mass flux:

$$\begin{aligned} \bar{J}_1^z &= \frac{1}{A} \int J_1^z dx dy \\ &= - \left[\frac{\int D_P(\mathbf{q}) \frac{\int d n_1(\mathbf{q})}{\int z} dx dy}{\int \frac{\int d n_1(\mathbf{q})}{\int z} dx dy} \right] \frac{1}{A} \int \frac{\int d n_1(\mathbf{q})}{\int z} dx dy \\ &= - \bar{D}_P(z) \frac{\int d \bar{n}_1(z)}{\int z} \end{aligned}$$

This expression is purely empirical and relies on considerations related to symmetries of the considered system.

Table 2. The self-diffusion coefficient of the pore nanofluid.

Pore section	Square channel	“Octahedron” section	Entire pore
Theoretical average value $D_P \cdot 10^4 \left(\frac{cm^2}{s} \right)$	0.483	1.232	0.894
NEMD value using Eqs. (15) and (16) $D_{NEMD} \cdot 10^4 \left(\frac{cm^2}{s} \right)$	0.57	0.76	-
$\frac{D_P - D_{NEMD}}{D_{NEMD}} \cdot 100\%$	-15.2	62.1	-

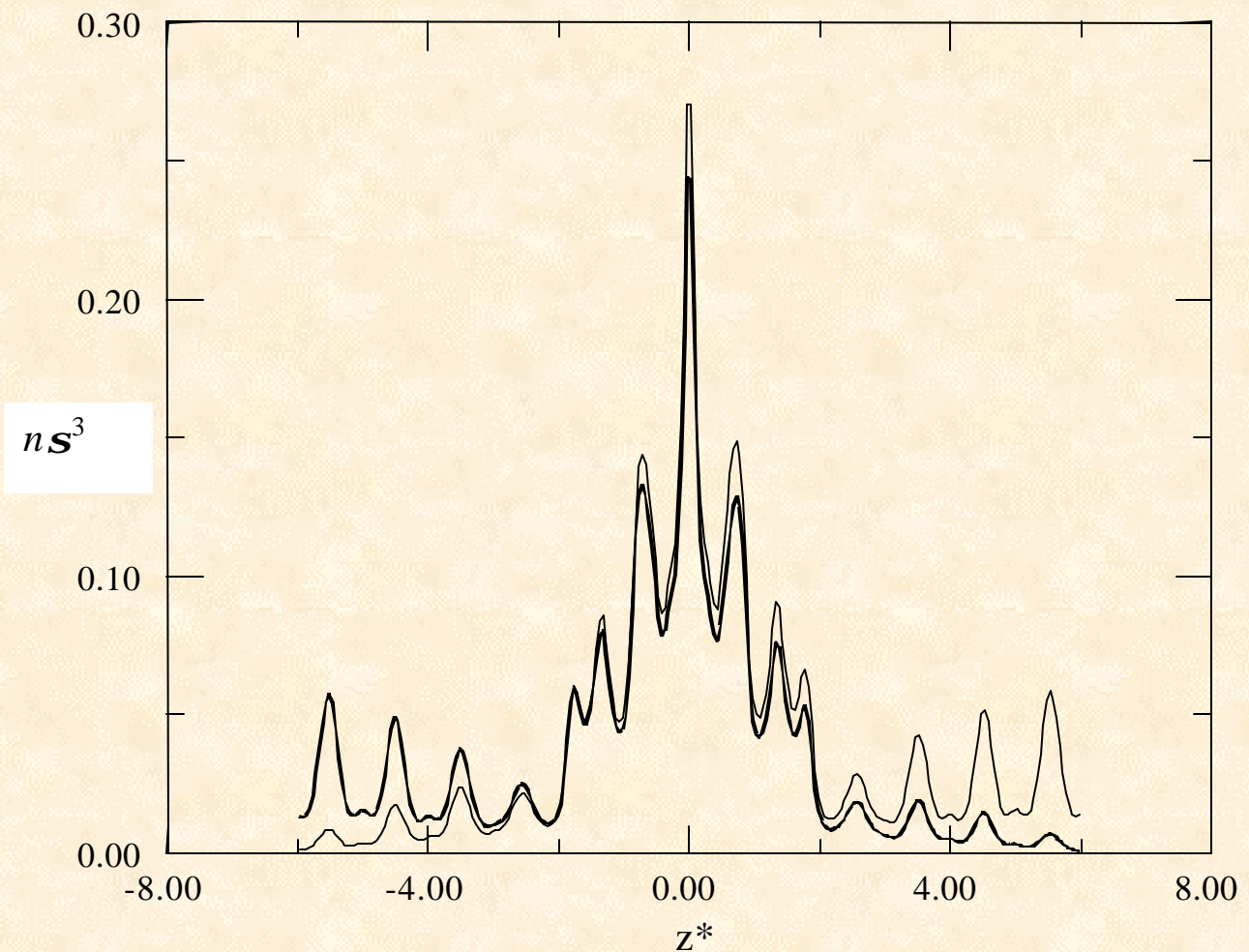


Figure 11. The non-equilibrium density profile of the counter-diffusing components expressed in the units of s^3 specific to the fluid atomic diameter; z^* is in units of $\sqrt{2}s_w$.

B) SHEAR VISCOSITY OF SLIT PORE NANOFUIDS

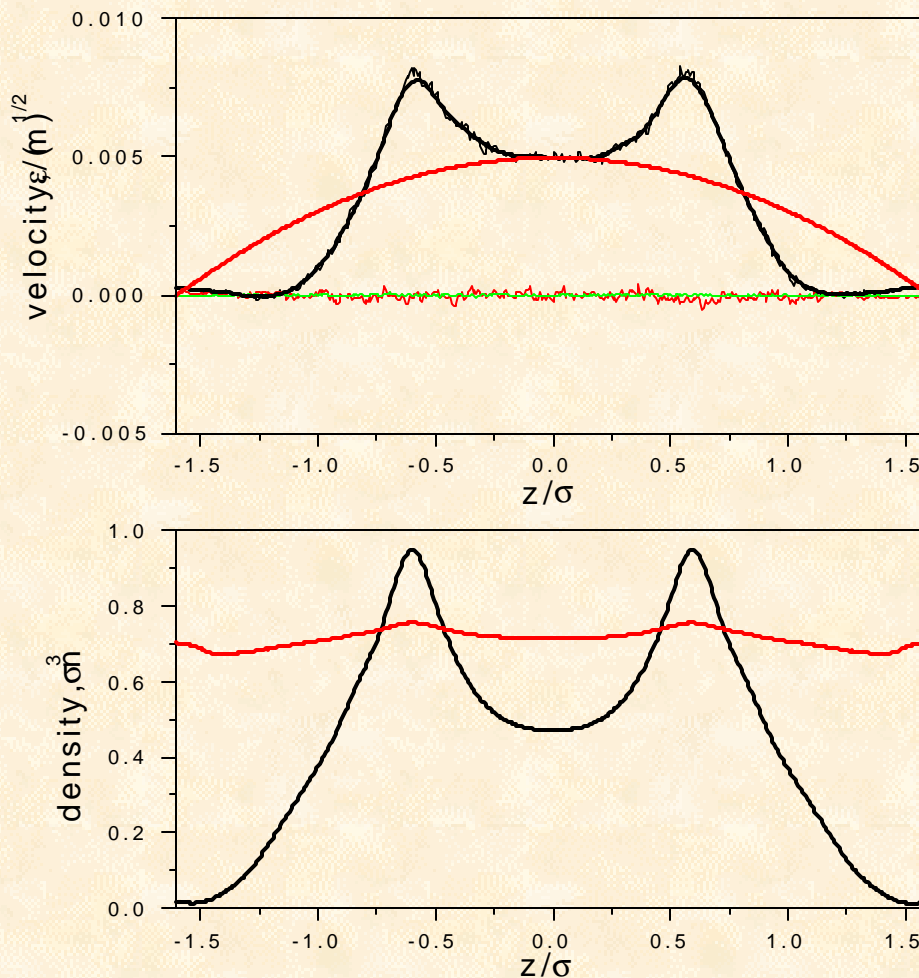


Figure. 12. Top: the NEMD velocity profile specific to the WCA fluid at $n\sigma^3=0.442$ and $k_B T/e=0.729$ confined in the pore of $H=3.2\sigma$ in width, and its “bulk” parabolic counterpart. Curve: the velocity component in the direction of the flow (y-direction); fluctuations: the velocity components in the x and z directions orthogonal to the flow direction. Bottom: the NEMD density and temperature (red curve).

“PRACTICAL” CORRELATION FOR THE SLIT PORE NANOFUID SHEAR VISCOSITY

“Standard” correlation between the average flow velocity, u_p , and the pressure gradient, dp/dy , specific to the Poiseuille flow of a “bulk” fluid between two parallel walls separated by the distance H (the parabolic velocity profile is assumed),

$$u_p = \frac{H^2}{12 h_p} \frac{dp}{dy} ,$$

η_p - fluid viscosity.

In these simulations of the Poiseuille flow of nanofluids $dp/dy = nF_e$, and therefore,

$$h_p = \frac{H^2}{12 u_p} nF_e .$$

COMMENT

The “local” heuristic definition of the viscosity,

$$h_{local}(z) = -\lim_{Fe \rightarrow 0} \left\{ \frac{\langle P_{yz}(z) \rangle}{\partial u_y / \partial z} \right\} ,$$

produces unphysical results (see References) and can not be used for the flows where the velocity profile features extrema (as is the case here).

Table 3. The PG-theoretical pore-average viscosity of pore nanofluids, h_{PG} [calculated from reduced PG-theoretical expression using EMD-simulated densities and pair correlation function contact values], and the 'NEMD + parabolic fit' pore-average viscosity, h_{fit} [calculated using parabolic fits to the NEMD data].

Pore width, Hs	Fluid average number density, ns^3	Temperature, $k_B T/e$	Parameter a/σ	Parameter b/σ	PG-theoretical pore-average viscosity, h_{PG}		'NEMD+ parabolic fit' pore-average viscosity, h_{fit}		Relative error, $\frac{h_{PG}-h_{fit}}{h_{fit}} \times 100\%$	
					WCA fluid	LJ fluid	WCA fluid	LJ fluid	WCA fluid	LJ fluid
3.2	0.442	0.729	2368	0.638	1.7569	2.0529	1.3760	1.9239	28	7
	0.442	0.729	2028	0.870	1.7736	1.9147	2.2813	3.2153	-22	-40
	0.442	0.729	1.933	0.958	2.1039	1.7976	2.6255	3.6767	-20	-51
	0.603	0.958	2028	0.870	7.9764	7.4496	N/A	N/A		
4.1	0.442	0.729	2339	0.654	1.3121	1.6355	1.1514	1.6919	14	-3
	0.603	0.958	2344	0.651	5.8127	5.1103	N/A	N/A		
5.1	0.442	0.729	2298	0.678	1.0571	1.3830	0.9422	1.6040	12	-14
	0.603	0.958	1.967	0.924	4.5466	4.1234	N/A	N/A		
7.0	0.442	0.729	2.265	0.698	0.7622	1.0934	0.7445	1.3299	2	-18
	0.603	0.958	1.934	0.952	3.2289	2.8812	N/A	N/A		

5. CONCLUSIONS

1. Virtual fabrication of structural nanomaterials is a cost-effective solution to a longstanding practical problem of development of nano- and sub-nano technologies for nanoheterostructure fabrication.
2. In addition to the above, virtual fabrication cycle allows to investigate transport processes at nanoscale (including quantum contributions) and to suggest and verify optimal parameters of the desirable nanomaterials to meet engineering and technological requirements.
3. Rigorous statistical mechanical theoretical approaches used in conjunction with EMD and, to some extent, with NEMD techniques, have to be used to facilitate virtual fabrication. At present, Pozhar-Gubbins approach is the most tractable among existing fundamental statistical mechanical approaches that can be used for this purpose.
4. Due to enhanced non-local nature of the transport coefficients in nanosystems (and possible large quantum contributions to them, in the case of quantum nanofluids) a heuristic analysis of molecular simulation data is unlikely to be helpful in conjunction with virtual fabrication of functional materials. In general, extreme care should be exercised when attempting to interpret local transport behaviour from coarse-grained data and/or heuristic evaluations.

ACKNOWLEDGEMENTS

This work was supported by the project No. KC0203020 from the Division of Material Sciences, Office of Science, the U.S. Department of Energy, through the contract No. DE-AC05-00OR22725. The authors thank J.M.D. MacElroy for fruitful collaboration, and E. Kontar for programming support.